Protein Tyrosine Phosphatase identification and profiling across liver disease progression.

Author: Elisavet Kalaitsidou
Examiner: Dr. Zhiyong Lei
Supervisor: Dr. Wei Wu
MSc Programme: Drug Innovation

Utrecht University

Singapore Immunology Network
SIgN

Table of Contents

List of abbreviations

DDA	Data Dependent Acquisition
DTT	Dithiothreitol
FDR	False Discovery Rate
HCC	Hepatocellular Carcinoma
HCD	High Energy Collision-Induced Dissociation
LC	Liquid Chromatography
LFQ	Label-Free Quantification
MS	Mass Spectrometry
MS/MS	Tandem Mass Spectrometry
NAFLD	Non-Alcoholic Liver Disease
NASH	Non-Alcoholic Steatohepatitis
NEM	N-ethylmaleimide
NCE	Normalized Collision Energy
NTPTP	Cytoplasmic or Non-Transmembrane PTP
PBMC	Peripheral Blood Monocytes
pKa	Dissociation Constant
PRM	Parallel Reaction Monitoring
PTK	Protein Tyrosine Kinases
PTP	Protein Tyrosine Phosphatases
PV	Pervanadate
QQQ	Quadrupole Mass Spectrometer
ROS	Reactive Oxygen Species
RPTP	Transmembrane or Receptor-like PTP
SRM	Selected Reaction Monitoring

Abstract

The phosphorylation of proteins on tyrosine residues is a critical post-translational modification, that can be rapidly reversed by protein tyrosine phosphatases (PTPs). Dysregulation of PTP enzyme family leads to abnormal levels of phosphorylation and subsequently can contribute to plethora of human diseases, including metabolic diseases, and cancers. The phosphatase activity of the classical cysteine-based PTPs depend on the essential cysteine within the conserved signature motif HCX_5R. Due to the low dissociation constant (pKa) of cysteine, it is maintained in the deprotonated state *in vivo*, rendering it susceptible to ROS-mediated oxidation. Oxidative inactivation of cysteine based PTPs, act as a general physiological mechanism for the regulation of PTP function and therefore in regulating signal transductions. In the present study, we define a method for the detection and identification of the reduced (active) and oxidized (inactive) forms of the PTPs in HeLa cell line and human derived liver tissues across the states of healthy liver, steatosis, NASH, HCC. Our established protocol involves chemical derivatisation to lock physiological redox-regulated PTP states, followed by antibody-based pulldown of hyperoxidized PTPs, in response to oxidizing agent pervanadate (PV). Subsequent sample analysis on LC-MS/MS in a DDA discovery mode and potentially in a PRM targeted mode to detect and quantify the relative proportion of reduced and oxidised PTPs. Proceeding from the UniProt database for the Human PTPs, containing the signature motif HCX_5R, we revealed the differential expression and oxidation of 21 unique human PTP proteins in liver tissue samples. Our method successfully identifies PTP, making it optimal for the further explorations of classical cysteine-based PTPs and demonstrate the broad utility of our MS-based PTP assay for human needle biopsies and other biological material to evaluate the intervention of PTPs in pathophysiological conditions.

Introduction

The physiological result is determined by the coordination of various interacting signaling networks, as opposed to earlier conception of signaling pathways as straightforward linear configurations of phosphorylation cascades that operate in isolation. The network of cellular protein tyrosine phosphorylation is balanced by the opposing functions of protein tyrosine kinases (PTKs) and protein tyrosine phosphatases (PTPs). Phosphorylation on tyrosine residues is mediated by PTKs, while removal of phosphorylation or dephosphorylation is performed by PTPs. Therefore, preserving the equilibrium between PTKs and PTPs is essential for the dynamic balance between the phosphorylated and dephosphorylated state of a signaling molecule[1,2]. Disruption of this equilibrium results in a myriad of pathophysiological conditions that can involve, cancers, metabolic diseases, and syndromes. Evidence raised in numerus publications highlight the importance of dephosphorylation and the regulatory role of PTPs. However, to assess the complicated network as well as multiple and intertwined roles of PTPs in various cell types and pathological conditions, it is vital to establish an approachable and optimal method for PTPs identification.

1.The diversity and structure of the PTP enzymes

Since the purification of the first PTP, PTP1B from the human placenta, 125 PTP genes have been identified in the human genome, including PTP and PTP-related proteins[3]. This number demonstrates the minimum degree of complexity in the family, as further multiplicity can be introduced through alternative promoters, mRNA splicing and post-translational modifications [2]. The catalytic residue that initiates the nucleophilic attack distinguish between cysteine-aspartic acid- or histidine-based phosphatases[3]. Based on the substrate specificity cysteine based PTP that contain the signature motif HCX_5R can be divided into IV subclasses[3]. We focus on the first subclass “the classical PTPs” that can dephosphorylate only tyrosine residues and can be further grouped in transmembrane or receptor-like PTPs and cytoplasmic or non-transmembrane PTPs[3].

21 transmembrane or receptor-like PTPs (RPTPs) are inserted in the plasma membrane, and comprise several extracellular domains, a transmembrane domain and a tandem (12), in some cases single (9) PTP domain. The membrane-proximal PTP domain (D1) and membrane-distal PTP domain (D2) or pseudo-phosphatase domain, serve a distinctive role[4]. The D1 domain is in charge for the catalytic activity of RPTPs, in contrast D2 domain is potentially inactive (apart from PTPα, where D2 show low activity[2]). However, structural integrity of the D2 domain is vital as it possess a regulatory role in dimerization or inactivation, substrate specificity, and redox sensing[5,6].

On the contrary a cytoplasmic or non-transmembrane PTPs (NTPTPs), possess only one PTP domain (D1), and their diversity resides within the non-catalytic regulatory domains such as SH2, PDZ, FERM, BRO1, that are located at the NH_2 or COOH terminus. The non-catalytic regulatory domains are important for the PTPs activity, substrate specificity, subcellular localization, and protein-protein interactions[7]. The absence of extracellular domains implies that NTPTPs function is independent of extracellular signals, while presence on RPTPs indicates the reliance on extracellular signal relay. Moreover many extracellular domains of RPTPs are similar in structure to the extracellular domains found in cell adhesion molecules suggesting the RPTPs involvement in cell–cell and cell–matrix contacts[2,4].

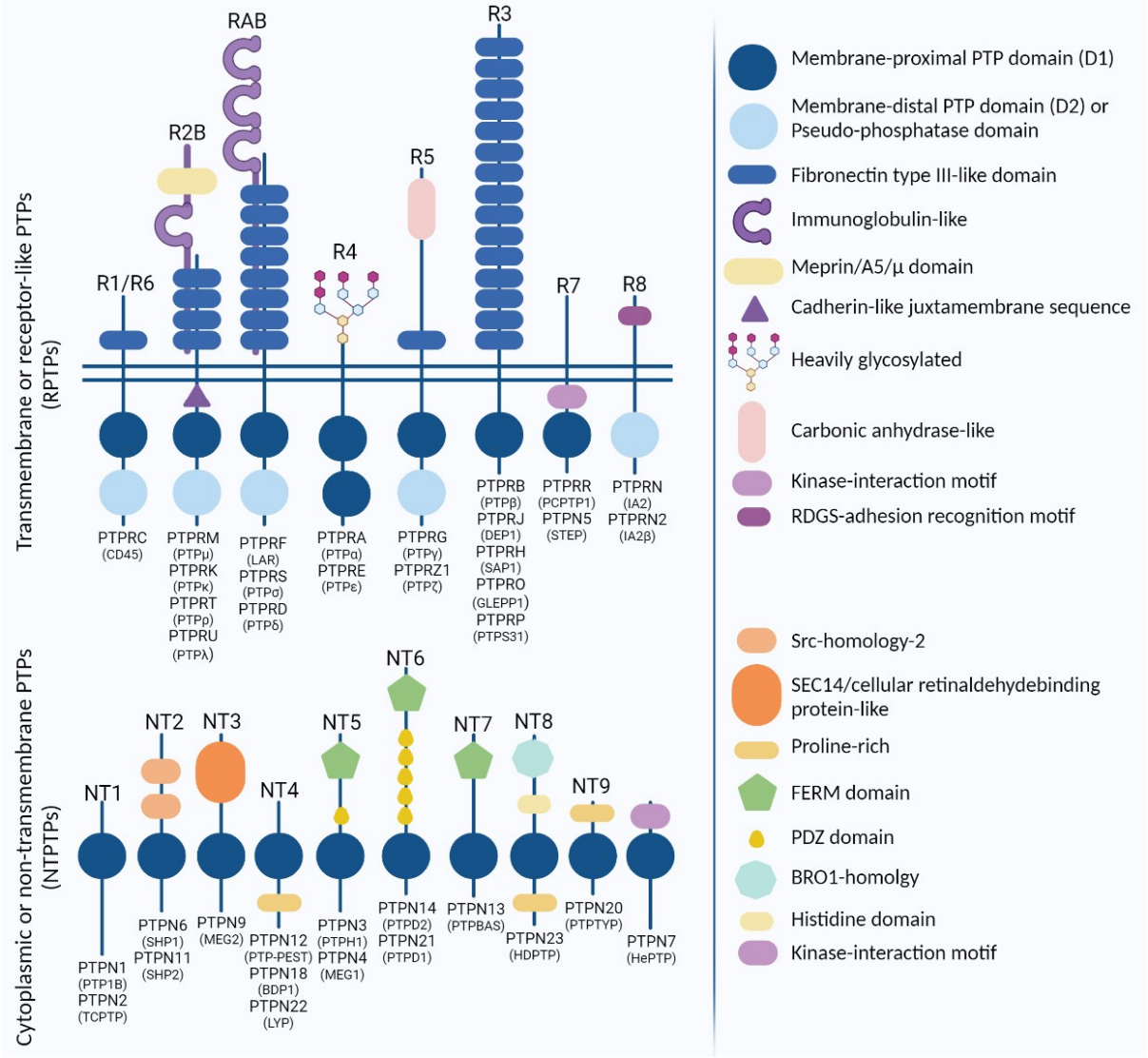

Fig. 1 | Cysteine-based PTPs: The subclass I or classical protein tyrosine phosphatases (PTPs) contain 37 PTPs. 16 non-transmembrane PTPs subdivided into nine types (NT1 to NT9), that possess only one PTP domain and multiple non-catalytic regulatory domains. 21 receptor-like PTPs (RPTPs) subdivided into eight types (R1/R6, R2a, R2b, R3, R4, R5, R7, and R8)[4], that contain two intracellular PTP domains, (PTP1/D1 or PTP2/D2), and multiple diverse extracellular domains with regulatory role.

Introduction

2.The catalytic reaction and oxidation

All classical cysteine based PTPs contain a highly preserved signature motif HCX_5R, also known as a P-loop, whereas cysteine is essential for the catalytic activity of the PTPs. The cysteine residue initiates the catalysis by the nucleophilic attack of the phosphorus atom of phosphorylated tyrosine residue, breaking the phosphorus-oxygen bond. Simultaneously, aspartate residue in the WDP-loop serves as a proton donor to the dephosphorylated tyrosine residue, while arginine nearby the P-loop facilitate stabilization and transition state of phosphate group. These events release the dephosphorylated tyrosine and produce phosphocysteine intermediate. Finally, the aspartate residue acts as a general base to remove a proton from a water molecule and facilitates the hydrolysis of the phosphorous-sulfur bond on phosphocysteine intermediate, resulting in the release of free phosphate[8,9].

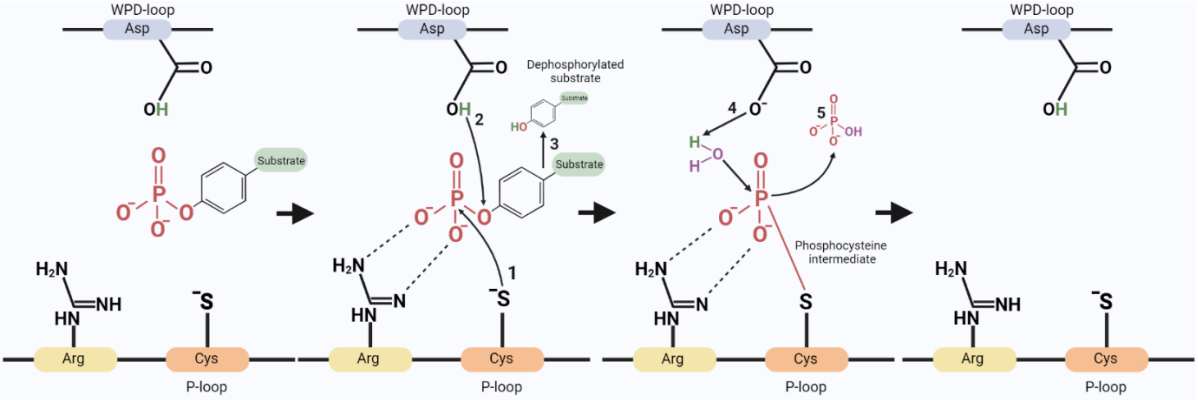

Fig. 2 | Catalytic mechanism of classical cysteine based PTPs. Numbers indicate the order of the steps, during reaction.

Cysteines of the classical PTPs, preserve a low dissociation constant (pKa), between 4.5 and 5.5 due to their microenvironment[6,10]. This characteristic allows the catalytic cysteine to remain at the thiolate anion state (S^-) at physiological pH, facilitating nucleophilic attack on phosphorylated tyrosine residues, although it also prone PTPs to ROS-mediated oxidation. Oxidation of the cysteine revoke its nucleophilic function and hence reduce or inhibit PTP activity. Upon oxidation of the active site, cysteine can be oxidized to the sulphenic acid form (SOH), which can be converted into sulfenylamide (-SN-) or cysteine disulfide (S-S) forms, to prevent further oxidation. Sulfenic, sulfenylamide and disulfide stages are reversible, as treatment with thiols lead to restoration of cysteine and PTP activity. In contrast, excessive oxidation to sulphinic (SO_2H) or sulphonic (SO_3H) acid forms, leads to catalytically inactive PTPs that cannot be restored[10–12]. Therefore, reversible oxidation can operate as a regulatory switch in the cells to maintain PTP activity within a certain range. Additionally this characteristic feature of PTPs can be utilized to detect oxidized and non-oxidized forms of PTPs upon treatment with the oxidizing agents, as antibodies specific for the oxidized to sulfonic acid (-SO_3H) form of cysteine are available on the current market.

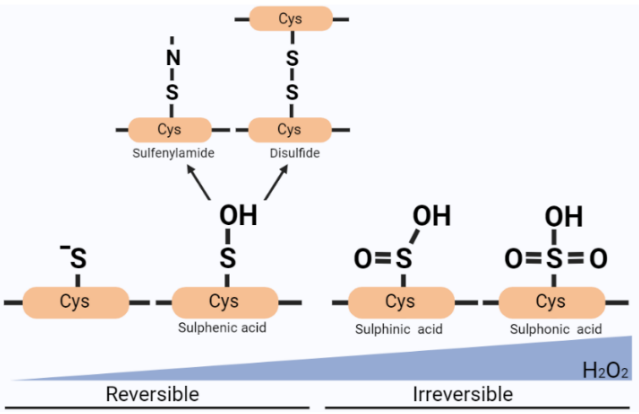

Fig. 3 | PTP state forms upon ROS-mediated oxidation.

Introduction

3. Obesity induced hepatocellular carcinoma (HCC)

Non-alcoholic fatty liver (NAFL) or steatosis, is a condition characterized by the excessive accumulation of lipids in lipid droplets in the cytosol of hepatocytes. NAFL development is associated with environmental and genetic factors and unrelated to excessive alcohol consumption or medications. Abnormal fat accumulation result in immune cells recruitment, leading to lipotoxicity and hepatocyte death, accelerating the progression to a more advanced condition termed non-alcoholic steatohepatitis (NASH). During NASH, hepatocyte death, inflammation and further immune cell recruitment exacerbate liver damage, promoting pathological healing, fibrogenesis and eventually fibrosis and cirrhosis. Fibrosis/cirrhotic patients are more likely to develop hepatocellular carcinoma (HCC), although, the process is not entirely understood. People with NASH can also develop HCC without fibrosis/cirrhosis stage, indicating potential non-direct association between steatosis, NASH, fibrosis/cirrhosis, and HCC.

4. Data-dependent acquisition (DDA) shotgun or discovery method

The most commonly used acquisition method in shotgun or discovery-based proteomics is a data-dependent acquisition (DDA). This method includes the acquisition of an MS scan or so-called survey scan in a high resolution. Peptides with higher intensity are subsequently subjected to further fragmentation for MS/MS acquisition. Traditionally, this technique is employed to compare different conditions across samples. Although it is ineffective in the consistent detection of proteins of interest across the samples or less abundant proteins in the sample, as peptides with higher intensity undergo fragmentation, DDA is optimal for protein identification in an unbiased manner, providing information that can be later on utilized to build targeted experiments[13–15].

5.Parallel reaction monitoring (PRM) targeted method

In contrast to the discovery-based proteomics that identifies proteins in unbiased manner, targeted methods, utilize a predefined m/z ranges of the peptides generated exclusively from the proteins of the interest. Resolving the problem of sporadic precursor selection in DDA. A relatively new SRM-like method known as parallel reaction monitoring (PRM) demonstrates performance on the next-generation mass spectrometers such as hybrid quadrupole-Orbitrap (q-OT), characterized by high resolution and mass accuracy. In q-OT, the preselected precursor ion is isolated in the first quadrupole (Q1) filter and transferred for the fragmentation in the high energy collision-induced dissociation (HCD) cell. From HCD cell the fragment ions are transferred and accumulate in the C-trap increasing signal-to-noise ratio of the ions, and finally injected and analysed in Orbitrap mass analyser[14,15]

The PRM method demonstrate several improvements over the traditional SRM targeted approach. PRM requires less method development, as preselection of optimal transitions is no needed. Therefore, higher specificity and identification of the peptide, can be obtained as all potential ion products/transitions of a target peptide are monitored. While ion accumulation in the C-trap offers higher ion availability for identification and high signal-to-noise/background ratio, which is less disruptive to overall spectral quality, leading to higher resolution of the PRM method[16–18]. Selection of the optimal surrogate peptide for the protein of the interest is a vital step in targeted methods like PRM. The properties that should be considered through the selection, determine reliable quantification of the protein of interest[18].

Results

1.Detection of PTP oxidation in Hela cell lysate

To assess the total number (active and inactive) and oxidized (inactive) PTPs in the HeLa cells, we utilized antibody-based methods. Under physiological conditions, PTPs within the cells are maintained at reduced state (PTP-S^-) and reversibly oxidized state (PTP-SOH). Therefore, HeLa cells were lysed in reducing or alkylated conditions to detect total and oxidized PTPs, respectively (Fig. 1.A.1.). Reducing agent dithiothreitol (DTT) in the lysis, followed by hyperoxidation with pervanadate (PV), transform all catalytic cysteines within the signature motif into catalytically inactive and irreversible form (SO_3H). Therefore an ox-PTP antibody, specific for the sulfonic acid (SO_3H) form of cysteine, enables the identification of total PTPs. On the other hand, identification of reversibly oxidized PTPs requires a different approach. First, reduced cysteines within the motif should be protected from the reducing agent and following hyperoxidation. Thus, an alkylation agent N-ethylmaleimide (NEM) is added to the lysis buffer, to alkylate all reduced cysteines (PTP-S^- → PTP-NEM). Afterwards, added DTT and PV agents reduce and hyperoxidize only oxidized PTPs, which can be detected by an ox-PTP antibody. This employed method[6,10,11,19] enables the identification of total PTPs and oxidized PTPs within the sample, whereas the evaluation of both reveals the level of active and inactive PTPs in HeLa cells.

Western Blot results demonstrated successful detection of total and oxidized PTPs in HeLa lysates (Fig. 4.B). Samples treated with DTT-PV to hyperoxidize total PTPs, appear with more bands, indicating the presence of multiple or total PTPs, in the HeLa lysate. On the contrary, in the NEM-DTT-PV treated sample, which aims to detect only oxidized PTPs, less bands are present. The comparison between these two samples correspond to PTPs that are maintained in the reduced form (active) in the cell. Noteworthy, PTPs are not the only proteins that contain cysteine at thiolate anion state (S^-), implying that treatment with PV may possibly hyperoxidize cysteines on other proteins, such as peroxidases and kinases[20–22]. Consequently, observed bands in PV treatment, potentially do not correspond only to the hyperoxidized PTPs.

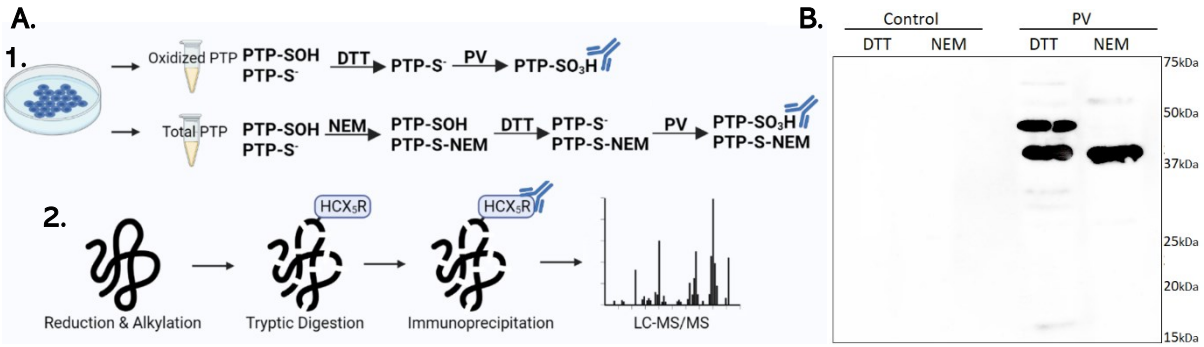

Fig. 4 | (A) Schematic workflow to detect total and oxidized PTP in HeLa lysates. (B) Western Blot result demonstrating the successful detection of total and oxidized PTPs in HeLa lysates. Lysates without PV treatments used as a control. Multiple bands are found in DTT-PV treated samples (correspond to total number of PTPs in HeLa cells), while NEM-DDT-PV sample appear with less bands (correspond to oxidized PTPs only). The presence of multiple bands within each row can be explained by the fact that PTP family consist of many PTPs that have distinct molecular weights and each of them can be hyperoxidized and subsequently detected by ox-PTP antibody. It is important to mention that PV hyperoxidize not only PTPs, but also other proteins, thus, multiple bands in both DTT-PV and NEM-PV treatments potentially may contain other proteins.

Results

2. Detection of PTP oxidation in human derived liver tissues

Following successful hyperoxidation and detection of total and oxidized PTPs in HeLa lysates, we proceeded with the human-derived liver biopsies. We were provided with 16 liver tissues samples representing four states of liver disease progression: 3 samples for the healthy liver, 4 samples for steatosis/ NAFL, 6 samples for NASH/cirrhosis/fibrosis, and 3 samples for the HCC. Each sample underwent the same treatment as HeLa lysates, for the PTP hyperoxidation and antibody-based detection. Western Blot (Fig. 5) results shown successful detection of total and oxidized PTPs in human-derived liver biopsies. Confirming that this method can find application not only in established cell lines, but also in tissue needle biopsies and potentially other biological materials.

Liver biopsies, demonstrate the same pattern of PTP expression as HeLa cells, upon treatment. Specifically, biopsies treated with DTT-PV appear with more bands, corresponding to the total number of PTPs in the sample. In contrast, biopsies treated with NEM-DTT-PV show fewer bands, corresponding only to oxidized PTPs. Certainly, not all observed bands belong to PTPs, other proteins could also be potential targets of hyperoxidation.

Interestingly, samples derived from patients with the steatosis and NASH/cirrhosis/fibrosis, demonstrate greater signal, in comparison to healthy and HCC samples. This indicate that as disease progress from healthy to fatty liver, more PTPs are present, although at the final stage HCC the presence of PTPs reduces. Additionally, we observe higher expression of oxidized PTP in NASH/ cirrhosis/fibrosis compared to other conditions. Recently it was observed that during NASH/ cirrhosis/fibrosis stage, more ROS are produced due to the hight immune cell infiltration and as it is known PTPs are target of ROS-mediated oxidation and therefore inactivation[23]. Consequently higher expression of oxidized PTP in NASH/ cirrhosis/fibrosis can be explained by the higher presence of ROS.

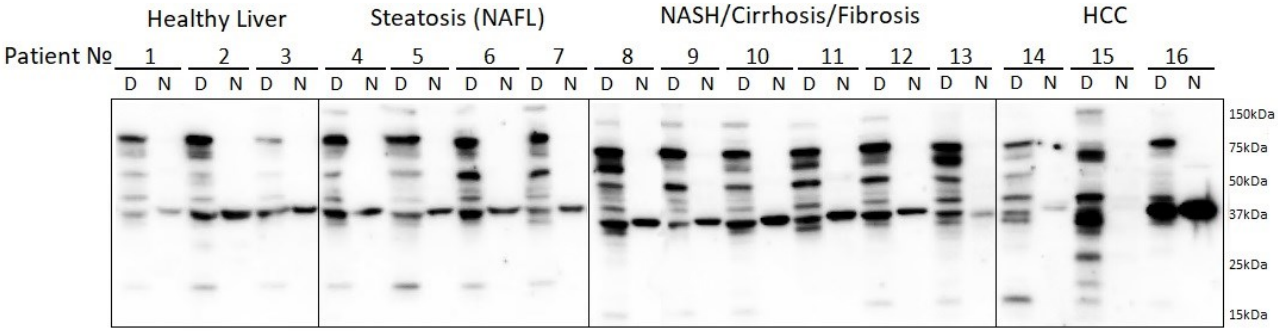

Fig. 5 | Western Blot result demonstrating the successful detection of total and oxidized PTPs in human-derived liver biopsies. All samples are treated with PV following DDT (indicated as D) or NEM (indicated as N) treatments. Multiple bands observed in D correspond to total number of PTPs. Few other proteins could be potentially included due to hyperoxidation of cysteine residue. Only one band is observed in N treatment, representing potentially only oxidized PTPs. Noteworthy to mention, that fatty liver (steatosis + NASH/cirrhosis/fibrosis) demonstrate elevated expression of PTP, revealing a PTP expression pattern across liver disease progression. Lastly, higher PTP oxidation and therefore inactivation, is detected in NASH/cirrhosis/fibrosis samples.

Results

3. Digestion, Immunoprecipitation, and PTP identification for human derived liver tissues

Following verification of PTP detection (total and oxidized) with antibody based-method, we proceed with the sample preparation as outlined in Fig. 4.A.2. for the following LC-MS/MS analyses in a DDA mode. Samples were enzymatically digested with Trypsin, that cleaves at C-terminal side after lysine and arginine (except when bound to a C-terminal proline). Digested peptides were purified using reverse-phase Sep-Pak C-18 to remove salts and buffers. Peptides containing hyperoxidized cysteine within the signature motif were eluted and followed immunoprecipitation with ox-PTP antibody. Subsequently, immunoprecipitated peptides were resuspended in 0.2% formic acid and injected in triplicate for the LC-MS/MS analyses.

Identification of PTPs was achieved using the preserved signature motif HCX_5R of every unique PTP peptide. In total ox-PTP immunoprecipitates, 18 distinct PTPs were identified. In contrast, previous studies for the PTP detection utilizing zebrafish fins, without the enrichment step, resulted in detection of 2698 proteins out of which only 2 were PTPs[6]. The immunoprecipitation with the ox-PTP antibody, resulted in high PTP enrichment, as we were able to identify 21 PTP motifs peptides, that are derived from 47 distinct PTP motifs peptides. We detected ~49% (18 of 37 PTP proteins) of all PTPs proteins expressed in human organism, demonstrating great detection improvement with ox-PTP immunoprecipitation. A representative spectrum obtained for the peptide from the PTPRA protein upon DTT-PV treatment is shown in Fig. 6, demonstrating high coverage with almost complete y- ion ladder.

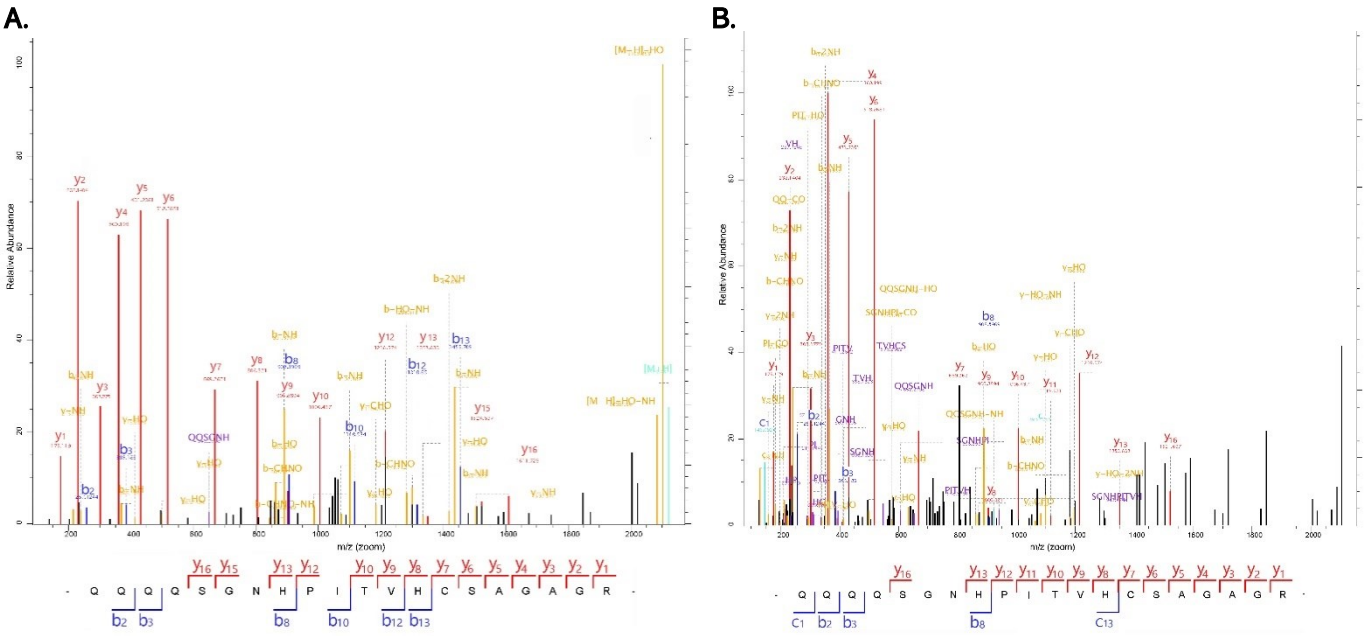

Fig. 6 |Two MS2 spectra were obtained for the -QQQSGNHPITVHCSAGAGR- peptide derived from the PTPRA phosphatase. Spectra are obtained from the steatosis and from the NASH/cirrhosis/fibrosis DTT-PV treated samples. Due to the trioxidation(O3) on the cysteine upon PV treatment, a slight mass shift is present. High coverage of the peptide with y-, b-, and c- ions, demonstrating reliance of the obtained data.

Results

Obtained results from the LC-MS/MS, were analysed and in total 21 HCX_5R motifs were identified from all 16 human-derived liver biopsies, which correspond to 18 distinct PTP proteins. While each sample exhibits a unique number of identified PTPs, within a particular liver disease stage they show similar PTP expression patterns. We generated a heatmap illustrating the PTP expression pattern across the states of a healthy liver, steatosis, NASH/cirrhosis/fibrosis, and HCC. The PTP in the heatmap are aligned from the high to low molecular weight, corresponding to RPTPs and NTPTPs respectively. With this alignment, it is easier to observe the specific pattern of PTPs as the liver disease progresses.

Heatmap indicates a reversed pattern of PTPs expression as the liver disease progress. In particular, RPTPs show high expression in healthy and especially in the steatosis and NASH/ cirrhosis/fibrosis samples, while in HCC they are completely absent. On the contrary, NTPTPs are present in HCC samples and almost non-existent in other conditions. Concluding, PTP seems to show a particular expression pattern as the liver disease progress, favouring the presence of the RPTPs in fatty liver and NTPTPs at a more advanced stage.

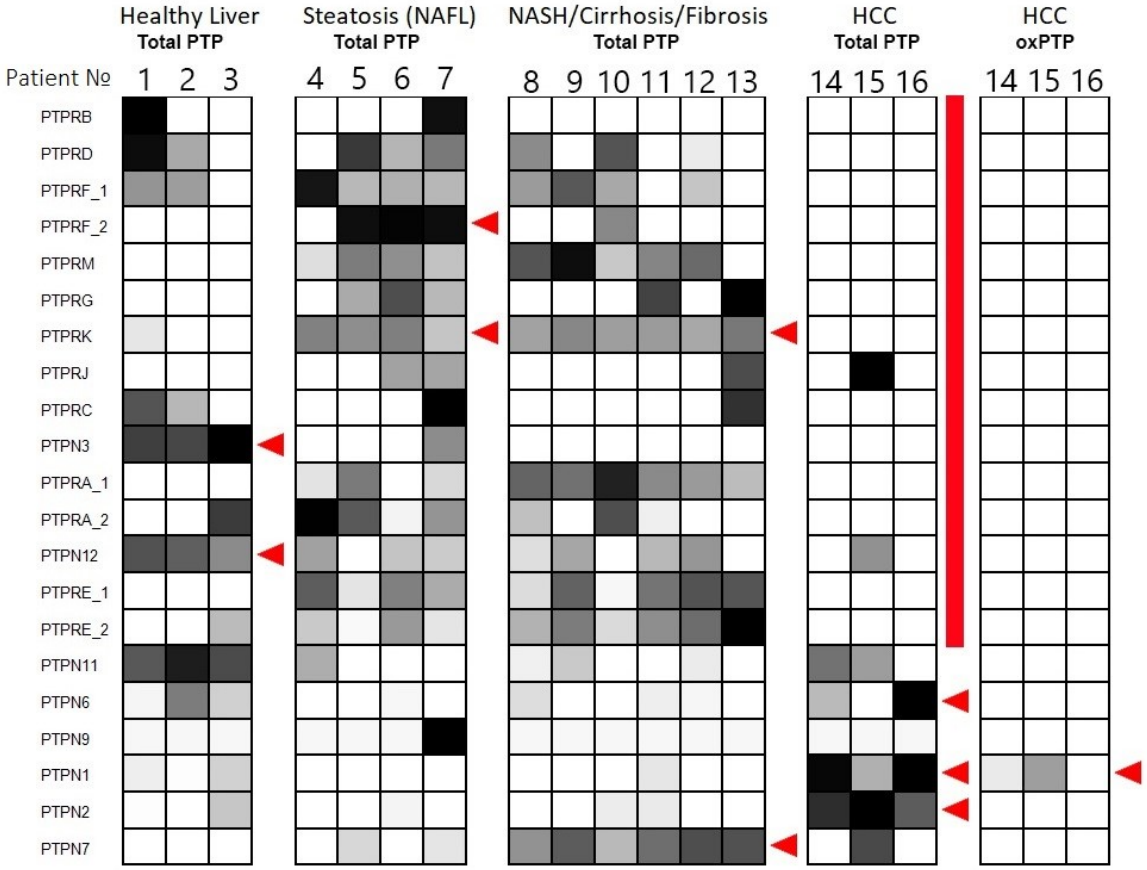

Fig. 7 | Heatmap for the PTP expression pattern across four states of liver disease progression. PTPs are lined up from the high to low molecular weight (from top to bottom). The colour intensity of the squares indicates the presence of the particular PTP in all three replicates (white: not present, light grey: present in one replicate dark grey: present in two replicates, black: present in three replicates). Red arrows indicate differential abundance of PTPs across different pathophysiological states.

Results

4. Alignment and masses estimation for the PRM targeted method

Proceeding from the published list of the extended human PTPome[3], we searched in the UniProt database for the reviewed (Swiss-Prot) Human PTPs, containing the signature motif HCX_5R that hold an essential cysteine. Considering that RPTPs contain tandem PTP domains, 47 signature motifs were found that correspond to 37 distinct PTPs. Hyperoxidation and antibody-based method described previously can detected all 37 PTPs. Noteworthy to mention that one PTP, PTPRN do not possess catalytic activity due to replacement of arginine with aspartic acid within the P-loop[24,25], leading to 36 enzymatically active PTPs.

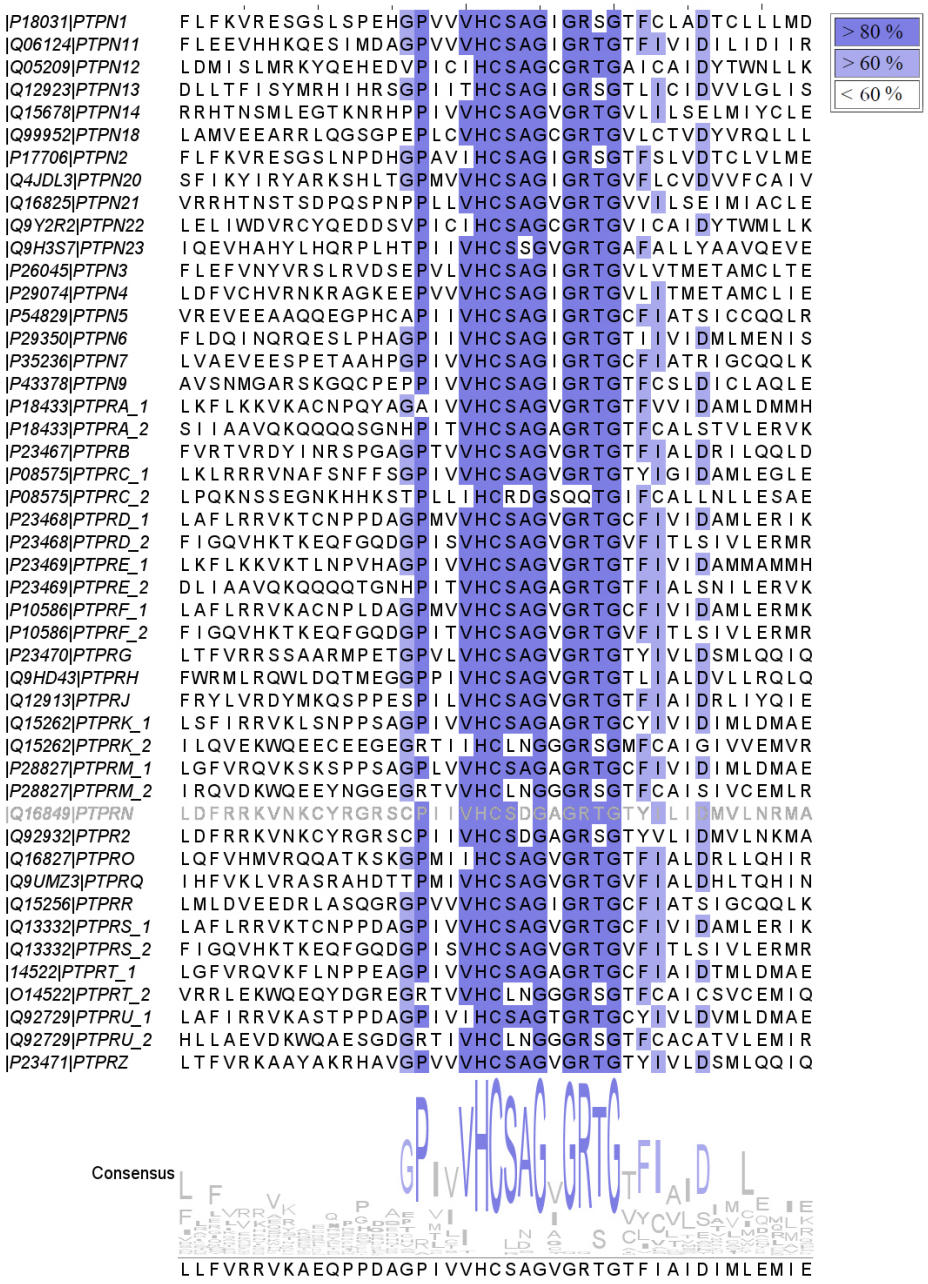

Fig. 8 | Clustal alignment of 47 PTPs catalytic sites with signature motif HCX_5R that contain an essential cysteine and 20 bordering amino acids. The height and the colour intensity of symbols in the sequence logo (consensus), illustrate relative frequency of particular residue at current position. Upper right box relates the intensity of the colour to the percentage of sequence conservation. Clustal alignment contain all 36 catalytically active human PTPs (black), one inactive PTP (grey) and 47 signature motifs. Image is generated in Jalview 2.11.2.4 software.

Results

Since we aim to utilize PRM targeted method to optimize and increase PTP detection, m/z of the peptides/precursor ions should be calculated. PTP sequences from the clustal alignment were used to generate *in silico* possible peptide sequences upon tryptic digestion. Consequently, peptides of 9 to 28 amino acids that hold the signature motif HCX_5R with an essential cysteine were chosen. Given that, PRM targeted method, requires masses (m/z) only for the precursor ions, we uploaded selected peptides to the Skyline software and calculated the masses (m/z) taking into consideration the fact that the cysteine residues within the peptides contains trioxidation modifiifation($-O_3$) group due to hyperoxidation. Generated m/z for the precursor ions, will be used along with the prepared samples for the future LC-MS/MS analysis.

Fig. 9 | Peptide sequences upon *in silico* tryptic digestion with the corresponding precursor ion masses. Data generated in Skyline 22.2.0.255 software.

Discussion and Future Outlook

Multiple research papers highlighted the important role of PTPs in human health, starting from early embryo development concluding with many pathophysiological conditions such as cancers, metabolic diseases, and syndromes. As our understanding of the physiological importance of PTPs has grown and continues to grow, so has our interest in PTP-based therapies. Although, the enormous potential for therapeutic interventions of the PTP, our understanding of this superfamily is still at the initial stage, as many enzymes remain uncharacterized in the context of their expression, regulation, and substrate specificity.

Our findings allowed us to propose an assumption that emphasizes the relationship between PTP expression and immune cell infiltration through the progression of liver disease. Abnormal fat accumulation during steatosis or NAFL leads to the recruitment of immune cells, which aim to restore disbalance in homeostasis. However, in case of immune cell incompetence, accumulated fat cause lipotoxicity and hepatocyte death, leading to further recruitment of immune cells. These events accelerate NAFL progression to NASH. During NASH, hepatocyte death and further immune cell recruitment exacerbate liver damage, resulting in pathological healing, and eventually fibrosis and cirrhosis[26]. Together, all these changes in the liver environment, favouring the emergence of HCC[23,27]. Interestingly, it was reported that HCC present low immune cell profile, due to low infiltration in comparison to prior stages and normal adjacent tissues[28]. Summarizing, we can illustrate a curve of immune cells infiltration pattern, with an increase as we progress from healthy liver to NAFL, NASH and fibrosis/cirrhosis, and decrease as disease terminate with HCC.

Remarkably, our findings involving RPTP expression demonstrate a consistent pattern with that of immune cells, throughout liver disease progression. In particular, RPTP expression on a protein level increase and culminate in NASH/cirrhosis/fibrosis and significantly drops in HCC. Moreover, PTPRD, PTPRF, PTPRH, PTPRO, and PTPRS were found to be downregulated or completely deficient in human HCC cell lines and tumor tissues on mRNA level[29]. This consistency in both patterns shows a direct relationship between RPTP and immune cells, raising an assumption that fluctuated RPTP expression may occur due to their expression on the immune cells within the liver. Little is known about the expression pattern of RPTP on immune cells on a protein level, especially in the context of liver disease progression. To this day the connection between RPTPs and immune cell infiltration has not been addressed or investigated, giving rise to more opportunities for further inspections.

The presence of the thiol anion on the catalytic cysteine, prone PTPs to ROS-mediated oxidation, which reversibly inhibit PTP functionality. This hypothetically demonstrates PTP enzymes as a target for the ROS-regulatory mechanisms. In fact, emerging contexts accept reversible oxidation as a general physiological mechanism for the regulation of PTP function. Only recently indirect ROS production by immune cell activity, was assigned to oxidize and inhibit PTP[23,31]. It was shown that in type 1 diabetes, elevated production of ROS mediated by infiltration of T-cells and macrophages into pancreatic islets, induce enhanced oxidation and hence PTP inactivation. This was the first indication of PTP inactivation upon immune infiltration in pancreas[30]. Following study, additionally demonstrated that obesity induced ROS production upon immune infiltration, inactivate PTPN2 promoting STAT1 or STAT3 signaling leading to HCC progression in two distinctive ways.

Besides, PTPs have an important role in co-ordinating the signaling networks that sustain lymphocyte homeostasis and regulate lymphocyte activation. From the list of over 100 cysteine based PTP genes, 58 to 76 are expressed in various immune cells, while about half of the classical PTPs are expresses on T cells. However, the majority of these PTPs on T cells seems to possess negative role in lymphocyte activation[32,33]. In fact mouse models, with chronic intestinal inflammation shown increase in disease exacerbation in the absence of PTPs, due to the hyper-activation of lymphocytes[34], while increased PTP oxidation has been demonstrated in human liver

biopsies from NAFLD patients[33]. However, little is known regarding PTP regulation on immune cells.

Currently, our findings, follow the concept of PTP oxidation in the presence of immune cells. Western Blotting (Fig.6) for the human-derived liver biopsies demonstrates high expression of the oxidized PTPs in the NASH/cirrhosis/fibrosis. Indicating, that high immune cell infiltration accompanying advanced stages of liver disease is straightforward with the PTP oxidation, potentially through ROS production.

Despite numerous publications, current studies do not provide the comprehensive expression profile of PTPs in various immune cells [35–38], as well as in other cell types, especially in relation to pathophysiological conditions. Considering our findings, we are confident that proteomic approaches can act as a steppingstone for the upcoming explorations of PTPs in human health. Based on antibody-based methods in combination with the MS-based approach, we were able to determine the expression pattern and the degree of oxidation of PTP, in human derived biopsies and established cell line. Demonstrating the remarkable potential of this application in multiple biological materials. Our current strategy involves two directions. Initially, we aim to optimize our approach, by utilizing the PRM targeted method. Resolving the problem of sporadic precursor selection in DDA, we expect to increase the detection capability to identify all possible PTPs. Next, step is to generate a PTP expression map in human derived peripheral blood monocytes (PBMCs). This map can be further compared with our data to reveal the relationship between PTP expression across different states of liver disease and immune cell infiltration. We are convinced, that our established technique for the PTP detection in response to PV in combination with the MS targeted method can find applications in multiple research questions and overcome potential challenges in current PTP studies.

Materials and methods

1.Cell Culture:

The human cervix adenocarcinoma HeLa cells obtained from the ATCC were cultured in RPMI-1640 (Cat. No. 31800022, Gibco) media supplemented with 10% fetal bovine serum (Cat. No. 10270106, Gibco), 1% L-Glutamine (Cat. No. 25030081, Gibco), and 1% penicillin-streptomycin (Pen-Strep). Cell cultures were maintained at 37°C in a humidified incubator with a 5% CO_2 air atmosphere. After reaching 80-90% confluence, the adherent cells were de-attached with 0.025% trypsin and passed in new plates.

2.Hela cells and liver biopsies lysis and hyperoxidation:

Two lysis Buffers were prepared. One comprising 8M Urea (Cat. No. BIO-2070, 1st Base), 50mM ammonium bicarbonate (Cat. No. A6141, Sigma), supplemented with protease inhibitor (Cat. No. 11836170001, Roche), phosphatase inhibitor (Cat. No. 4906845001, Roche), DNAse (Cat. No. DN25, Sigma), RNAse (Cat. No. R6513, Sigma), Sodium deoxycholate (Cat. No. 30970, Sigma) and dithiothreitol (DTT) (Cat. No. 22C1456434, VWR) for the total number of PTPs. Another lysis contained N-Ethylmaleimide (NEM) (Cat. No. E3876, Sigma) as a replacement for of DTT, for the oxidized PTPs. HeLa cell pellets and minced liver biopsies were separated equally in two eppendorfs and lysed in described lysis buffers. Liver biopsies were ultra-sonicated for 10sec with 30% amplitude of 7 duty cycles (Branson digital sonifier 450). All lysates were centrifuged at 16.000g for 1hour at RT. Supernatants were collected and DTT reducing agent was added to the NEM contained lysates. Protein concentration of the supernatants was determined by Bradford protein assay (Cat. No. 5000205, Bio-Rad). 700ug of each sample underwent a buffer exchange with centrifugal filter units 3K (Cat. No. UFC500396) to remove Urea from the samples. Protein concentration was determined to establish the percentage of protein loss. Buffer exchanged samples were subsequently hyperoxidized with 1mM pervanadate 8.5 mM H_2O_2 and 1mM Sodium Orthovanadate (Cat. No. 13721396, Santa Cruz), mixed and left at 4°C overnight.

3.Western Blotting for oxidation validation:

To evaluate PTP oxidation, 5 mg of protein from each sample (before and after hyperoxidation), was denatured by boiling in Laemmli Sample Buffer (Cat. No. 1610747, Bio-Rad) containing 200nM DTT. Proteins were resolved on 12% acrylamide gel (Cat. No. 1610149, Bio-Rad) at a constant of 10mA for 30 min, followed by 15mA till desirable. Proteins were transferred onto a PVDF membranes (Cat. No.1620177, Bio-Rad) by wet-tank transfer at 100 V for 1 hour at 4°C in transfer buffer (10% 25 mM Tris, 192 mM glycine, 20% (v/v) methanol, 70% MiliQ (pH 8.3). The membranes were blocked for 1 hour at room temperature with 5% non-fat dried milk in tris-buffered saline containing 0.1% Tween 20 (TBST 1X) and incubated overnight at 4°C with an oxidized PTP active site antibody (Cat. No. MAB2844, R&D Systems) diluted at 1:2000 ratio in 1% non-fat dried milk in TBST 1X. After overnight incubation with the antibody, the membranes were washed X3 times for 5 minutes in TBST 1X on the orbital shaker and then incubated for 1 hour at room temperature with HRP-conjugated anti-mouse secondary antibody (Cat. No, NA931VS, Cytiva) diluted at 1:5000 ratio in 1% milk in TBST 1X. SuperSignal West Dura (Cat. No. WK340468, Thermo Scientific) chemiluminescent substrate was prepared at the 1:1 ratio and poured on the membrane. The signal was detected using an ChemiDoc Imaging system (Bio-Rad).

Materials and methods

4.Hela cells and liver biopsies digestion and purification:

Following hyperoxidation validation, hyperoxidized proteins of each lysate were mixed with 120ug Urea, and 0.3ul NaOH to obtain pH 8. The derivatized samples were reduced in 4mM DTT at 20°C for 1h and then alkylated in 8mM iodoacetamide (IAA) at 20°C for 30min in the dark. For the subsequent protein digestion, trypsin was added at 1:100 ratio overnight at 37°C, followed by additional two digestions with trypsin at 1:200 ratio for 4h each at 37°C. An SDS-Page was performed to verify tryptic peptides digestion.

To purify digested peptides from salts, reverse-phase Sep-Pak 1cc (50mg) C18 cartridges (Cat. No. 045132007A, Waters) were utilized. Samples were diluted with 100% and 0.1M acetic acid to obtain pH 3 and total volume of 1ml. Initially, columns were activated with 100% acetonitrile (ACN) and equilibrated with 0.1% acetic acid. Sample were loaded on the column and left to run through, the flow through was collected and stored at -80°C. C18 columns were washed once with acetic acid, and peptides were eluted twice with 300 µl 80% ACN and 0.1M acetic acid. Both eluates were combined and dried by vacuum centrifugation.

5.Immuno-affinity purification (IAP) of hyperoxidized peptides:

10ug of oxidized PTP active site antibody was bound to protein A/G plus agarose in the column, following by crosslinking to prevent antibody co-elution (Cat. No. 26147, Thermo Scientific). Hyperoxidized peptides, were added onto the antibody - A/G agarose containing columns. Incubation was performed overnight at 4°C with end-to-end rotation. On the next day, flow through was collected, and hyperoxidized peptides were eluted with 30ul of 10% acetic acid. The resin was washed X3 times with PBS 1X and previously collected flow through was added to the column for additional X4 incubation of 4h at 4°C with end-to-end rotation. All five eluates were collected in the same tube with total volume of 150ul. All samples were dried by vacuum centrifugation and stored at -80°C for mass spectrometry analyses.

6.LC-MS/MS and raw data analysis:

Pulled down PTP peptides with the signature motif HCX_5R, were reconstituted in 2% formic acid and separated on a 40-min reverse-phase gradient on the UHPLC 1290 system (Agilent), with the following analysis on an Orbitrap Q Exactive HF mass spectrometer (Thermo Scientific). Peptides were first trapped on a HPLC pre-column (Reprosil C18, 3 µm, 2cm × 100 µm), and then separated on an analytical column (Poroshell EC-C18, 2.7 µm, 50 cm × 75 µm). Flow rate was kept at 300 nl/min. Peptides were trapped for 5min in Solvent A (0.1 M acetic acid in MiliQ) and eluted with Solvent B (80% ACN in 0.1 M acetic acid) by 20min gradient from 13 to 44%, followed by 3min gradient from 44 to 100% and finally equilibrating back to Solvent A for 10 min.

PTP peptides were online injected in the mass spectrometer and the MS data were obtained in the DDA mode. MS scans were acquired at the resolution of 60,000 in the m/z range of 375–1500, with the pre-set automated gain control (AGC) target. Top 7 most intense precursor ions were selected for HCD fragmentation performed at 27% NCE, after accumulation to target value of 1E5, also in a maximum injection time of 150ms. MS/MS acquisition was performed at a resolution of 30,000 in the 1.4 m/z range, and dynamic exclusion was set to 6.0 s.

MS data was acquired with Thermo Scientific Xcalibur (version 4.4.16.14) and spectral files were processed using MaxQuant (version 2.0.3.0) and searched against the *Homo Sapiens* Uniprot database (downloaded in August 2022) with the integrated Andromeda search engine. LFQ was enabled, cysteine carbamidomethylation was settled as a fixed modification, while trypsin as a digest enzyme. Variable modifications of methionine oxidation, cysteine hyperoxidation, and < 2 missed cleavages were tolerated. For protein and peptide identification a false discovery rate (FDR) was restricted to 1%.

7.Data analysis and statistics:

The provided data was analysed using Microsoft Excel and Perseus software (version 1.6.15.0) and GraphPad Prism (version 8.0). Intensities of proteins were log2 transformed. Spectra obtained in three replicate MS runs were summed and averaged. To filter for statistically significant changes between experimental conditions two-sided unpaired Student's t test was performed. FDR-corrected p-values or in other words q-values were calculated from 250 randomisations and S0 = 0, were considered statistically significant if ≤ 0.05.

8.PTP peptides generation and m/z calculation:

To generate *in silico* peptides containing the signature motif HCX_5R that hold an essential cysteine, we searched against the reviewed human PTPs in UniProt database (released in March 2022). All 47 PTP sequences that correspond to 37 PTPs, were aligned in Jalview software (version 2.11.2.4), with the focus on the signature motif and 20 bordering amino acids from both directions. Subsequently, sequences from the alignment were *in silico* digested with trypsin in Skyline software (version 22.2.0.255) to generate peptides of 9-28 amino acids. Peptides that hold the signature motif were selected.

The sequences of selected peptides were uploaded to the Skyline software (version 22.2.0.255). Since we upload only peptide sequences of the interest there is no need to adjust any setting for the digestion Cysteines were modified to carry a trioxidation (O_3) due to hyperoxidation. The retention time values are left on default. Skyline automatically generate optimal charge and m/z ratio of the precursor ions, that can be directly uploaded on the Skyline software for MS analysis in PRM mode.

References:

1. Lee C, Rhee I. Important roles of protein tyrosine phosphatase PTPN12 in tumor progression. *Pharmacol Res*. 2019;144(March):73-78. doi:10.1016/j.phrs.2019.04.011

2. Tonks NK. Protein tyrosine phosphatases: From genes, to function, to disease. *Nat Rev Mol Cell Biol*. 2006;7(11):833-846. doi:10.1038/nrm2039

3. Alonso A, Pulido R. The extended human PTPome: A growing tyrosine phosphatase family. *FEBS Journal*. 2016;283(8):1404-1429. doi:10.1111/febs.13600

4. Lee H, Yi JS, Lawan A, Min K, Bennett AM. Mining the function of protein tyrosine phosphatases in health and disease. *Semin Cell Dev Biol*. 2015;37:66-72. doi:10.1016/j.semcdb.2014.09.021

5. Hay IM, Fearnley GW, Rios P, Köhn M, Sharpe HJ, Deane JE. The receptor PTPRU is a redox sensitive pseudophosphatase. *Nat Commun*. 2020;11(1). doi:10.1038/s41467-020-17076-w

6. Wu W, Hale AJ, Lemeer S, den Hertog J. Differential oxidation of protein-tyrosine phosphatases during zebrafish caudal fin regeneration. *Sci Rep*. 2017;7(1):1-9. doi:10.1038/s41598-017-07109-8

7. Soulsby M, Bennett AM. Physiological signaling specificity by protein tyrosine phosphatases. *Physiology*. 2009;24(5):281-289. doi:10.1152/physiol.00017.2009

8. Zhao S, Sedwick D, Wang Z. Genetic alterations of protein tyrosine phosphatases in human cancers. *Oncogene*. 2015;34(30):3885-3894. doi:10.1038/onc.2014.326

9. Cho, Possomato-Vieira, José S. and Khalil RAK. 乳鼠心肌提取 HHS Public Access. *Physiol Behav*. 2016;176(1):139-148. doi:10.1038/onc.2014.326.Genetic

10. Karisch R, Neel BG. Methods to monitor classical protein-tyrosine phosphatase oxidation. *FEBS Journal*. 2013;280(2):459-475. doi:10.1111/j.1742-4658.2012.08626.x

11. Weibrecht I, Böhmer SA, Dagnell M, Kappert K, Östman A, Böhmer FD. Oxidation sensitivity of the catalytic cysteine of the protein-tyrosine phosphatases SHP-1 and SHP-2. *Free Radic Biol Med*. 2007;43(1):100-110. doi:10.1016/j.freeradbiomed.2007.03.021

12. Choi S, Love P. Detection of Intracellular Reduced (Catalytically Active) SHP-1 and Analyses of Catalytically Inactive SHP-1 after Oxidation by Pervanadate or H2O2. *Bio Protoc*. 2018;8(1):1-10. doi:10.21769/bioprotoc.2684

13. Cottrell JS. Protein identification using MS/MS data. *J Proteomics*. 2011;74(10):1842-1851. doi:10.1016/j.jprot.2011.05.014

14. Schmidlin TT. *Novel Methods and Applications of Data-Independent and Targeted Mass Spectrometry ; Towards Robust Quantification of Molecular Signaling Events*.

15. Rauniyar N. Parallel reaction monitoring: A targeted experiment performed using high resolution and high mass accuracy mass spectrometry. *Int J Mol Sci*. 2015;16(12):28566-28581. doi:10.3390/ijms161226120

References:

16. Peterson AC, Russell JD, Bailey DJ, Westphall MS, Coon JJ. Parallel reaction monitoring for high resolution and high mass accuracy quantitative, targeted proteomics. *Molecular and Cellular Proteomics*. 2012;11(11):1475-1488. doi:10.1074/mcp.O112.020131

17. van Bentum M, Selbach M. An Introduction to Advanced Targeted Acquisition Methods. *Molecular & Cellular Proteomics*. 2021;20:100165. doi:10.1016/j.mcpro.2021.100165

18. 1.8.Parallel Reaction Monitoring (GOOD ONE).pdf.

19. Huyer G, Liu S, Kelly J, et al. Mechanism of inhibition of protein-tyrosine phosphatases by vanadate and pervanadate. *Journal of Biological Chemistry*. 1997;272(2):843-851. doi:10.1074/jbc.272.2.843

20. Nelson KJ, Parsonage D, Karplus PA, Poole LB. Evaluating peroxiredoxin sensitivity toward inactivation by peroxide substrates. *Methods Enzymol*. 2013;527(Figure 1):21-40. doi:10.1016/B978-0-12-405882-8.00002-7

21. Randall LM, Ferrer-Sueta G, Denicola A. *Peroxiredoxins as Preferential Targets in H2O 2-Induced Signaling*. Vol 527. 1st ed. Elsevier Inc.; 2013. doi:10.1016/B978-0-12-405882-8.00003-9

22. Nelson KJ, Bolduc JA, Wu H, et al. H2O2 oxidation of cysteine residues in c-Jun N-terminal kinase 2 (JNK2) contributes to redox regulation in human articular chondrocytes. *Journal of Biological Chemistry*. 2018;293(42):16376-16389. doi:10.1074/jbc.RA118.004613

23. Brahma MK, Gilglioni EH, Zhou L, Trépo E, Chen P, Gurzov EN. Oxidative stress in obesity-associated hepatocellular carcinoma: sources, signaling and therapeutic challenges. *Oncogene*. 2021;40(33):5155-5167. doi:10.1038/s41388-021-01950-y

24. Magistrelli G, Toma S, Isacchi A. Substitution of Two Variant Residues in the Protein Tyrosine Phosphatase-like PTP35 / IA-2 Sequence Reconstitutes Catalytic Activity PTPases may exist as cytoplasmic as well as transmembrane molecules , all possessing one or two highly conserved regions o. 1996;588:581-588.

25. Notkins AL. Immunologic and genetic factors in type 1 diabetes. *Journal of Biological Chemistry*. 2002;277(46):43545-43548. doi:10.1074/jbc.R200012200

26. Hirsova P, Bamidele AO, Wang H, Povero D, Revelo XS. Emerging Roles of T Cells in the Pathogenesis of Nonalcoholic Steatohepatitis and Hepatocellular Carcinoma. *Front Endocrinol (Lausanne)*. 2021;12(October):1-14. doi:10.3389/fendo.2021.760860

27. Elvira B, Vandenbempt V, Bauzá-Martinez J, et al. PTPN2 Regulates the Interferon Signaling and Endoplasmic Reticulum Stress Response in Pancreatic β-Cells in Autoimmune Diabetes. *Diabetes*. 2022;71(4):653-668. doi:10.2337/db21-0443

28. Bian J, Lin J, Long J, et al. T lymphocytes in hepatocellular carcinoma immune microenvironment: insights into human immunology and immunotherapy. *Am J Cancer Res*. 2020;10(12):4585-4606.

29. Huang Y, Zhang Y, Ge L, Lin Y, Kwok HF. The roles of protein tyrosine phosphatases in hepatocellular carcinoma. *Cancers (Basel)*. 2018;10(3):1-21. doi:10.3390/cancers10030082

References:

30. Stanley WJ, Litwak SA, Quah HS, et al. Inactivation of protein tyrosine phosphatases enhances interferon signaling in pancreatic islets. *Diabetes*. 2015;64(7):2489-2496. doi:10.2337/db14-1575

31. Dias VJ, Mouradian E. 基因的改变 NIH Public Access. *Bone*. 2008;23(1):1-7. doi:10.1016/j.cmet.2014.05.011.Hepatic

32. Arimura Y, Yagi J. Comprehensive expression profiles of genes for protein tyrosine phosphatases in immune cells. *Sci Signal*. 2010;3(137):1-11. doi:10.1126/scisignal.2000966

33. Grohmann M, Wiede F, Dodd GT, et al. Obesity Drives STAT-1-Dependent NASH and STAT-3-Dependent HCC. *Cell*. 2018;175(5):1289-1306.e20. doi:10.1016/j.cell.2018.09.053

34. Pike KA, Tremblay ML. Protein Tyrosine Phosphatases: Regulators of CD4 T Cells in Inflammatory Bowel Disease. *Front Immunol*. 2018;9(October):1-14. doi:10.3389/fimmu.2018.02504

35. 3. Protein Tyrosine Phosphatase PTPRS Is an Inhibitory Receptor on Human and Murine Plasmacytoid Dendritic Cells _ Enhanced Reader.pdf.

36. Pike KA, Tremblay ML. Protein Tyrosine Phosphatases: Regulators of CD4 T Cells in Inflammatory Bowel Disease. *Front Immunol*. 2018;9(October):1-14. doi:10.3389/fimmu.2018.02504

37. Zhang W, Liu Y, Yan Z, et al. IL-6 promotes PD-L1 expression in monocytes and macrophages by decreasing protein tyrosine phosphatase receptor type O expression in human hepatocellular carcinoma. *J Immunother Cancer*. 2020;8(1):1-14. doi:10.1136/jitc-2019-000285

38. Al Barashdi MA, Ali A, McMullin MF, Mills K. Protein tyrosine phosphatase receptor type C (PTPRC or CD45). *J Clin Pathol*. 2021;74(9):548-552. doi:10.1136/jclinpath-2020-206927